



Phenomena of electrostatic perturbations before strong earthquakes (2005–2010) observed on DEMETER

X. Zhang¹, X. Shen¹, M. Parrot², Z. Zeren¹, X. Ouyang¹, J. Liu¹, J. Qian¹, S. Zhao¹, and Y. Miao¹

¹Institute of Earthquake Science, CEA, Beijing 100036, China

²LPC2E/CNRS, 3A Avenue de la Recherche Scientifique, 45071 Orléans cedex 2, France

Correspondence to: X. Zhang (zhangxm69@yahoo.cn)

Received: 27 October 2010 – Revised: 30 November 2011 – Accepted: 5 December 2011 – Published: 9 January 2012

Abstract. During the DEMETER operating period in 2004–2010, many strong earthquakes took place in the world. 69 strong earthquakes with a magnitude above 7.0 during January 2005 to February 2010 were collected and analysed. The orbits, recorded in local nighttime by satellite, were chosen by a distance of 2000 km to the epicentres during the 9 days around these earthquakes, with 7 days before and 1 day after. The anomaly is defined when the disturbances in the electric field PSD increased to at least 1 order of magnitude relative to the normal median level about $10^{-2} \mu\text{V}^2/\text{m}^2/\text{Hz}$ at 19.5–250 Hz frequency band, and the starting point of perturbations not exceeding 10° relative to the epicentral latitude. Among the 69 earthquakes, it is shown that electrostatic perturbations were detected at ULF-ultra low frequency and ELF-extremely low frequency band before the 32 earthquakes, nearly 46%. Furthermore, we extended the searching scale of these perturbations to the globe, and it can be found that before some earthquakes, the electrostatic anomalies were distributed in a much larger area a few days before, and then they concentrated to the closest orbit when the earthquake would happen one day or a few hours later, which reflects the spatial developing feature during the seismic preparation process. The results in this paper contribute to a better description of the electromagnetic (EM) disturbances at an altitude of 660–710 km in the ionosphere that can help towards a further understanding of the lithosphere-atmosphere-ionosphere (LAI) coupling mechanism.

1 Introduction

Spatial electromagnetic phenomena have been widely observed by satellites, including the anomalies in the electric field, magnetic field, plasma parameters and energetic par-

ticles (Pulinets and Boyarchuk 2004; Zhang et al., 2007; Anagnostopoulos and Rigas, 2009). Ionospheric anomalies attract more and more attention nowadays by their short-term feature, for they always occur one week before earthquakes. A lot of statistical analysis has shown the correlation between the electric field anomalies in the ionosphere and strong earthquakes. An anomalous increase in the intensity of low-frequency (0.1–16 kHz) radiowave emissions was detected by using Intercosmos-19 data (Larkina et al., 1989). Parrot and Mogilevsky (1989) studied the GEOS and AUREOL-3 satellite data and they found that earthquakes caused extremely low frequency electromagnetic emissions in the upper ionosphere. Parrot (1994) analysed the AUREOL-3 satellite data of around 325 earthquakes with $M_s > 5$. His results showed that during a 24-h window, the maximum amplitude in the electric field occurred in the interval of $\Delta\text{Lon} < 10^\circ$ ($\text{Lon} \sim$ longitude) from the epicentres regardless of $\Delta\text{Inv.lat}$ ($\text{Inv.lat} \sim$ invariant latitude). Molchanov et al. (1993) summarized the 28 earthquakes occurring during 16 November 1989 to 31 December 1989, based on Intercosmos-24 satellite data. They found that emissions with a spectrum maxima were observed at ULF-ELF (f less than 1000 Hz) over the epicentral areas and these emissions were mainly observed at 12–24 h before the main shocks. Serebryakova et al. (1992) found similar EM radiations on satellites COSMOS-1809 and AUREOL-3 with a frequency below 450 Hz over the seismic region in Armenia before strong earthquakes during 20 January to 17 February 1989. Gousheva et al. (2008) presented their results of anomalies in the quasi-static electric field in the upper ionosphere ($h = 800$ – 900 km) observed by the satellite INTECOSMOS-BULGARIA-1300 over seismic regions and found the increase in the vertical component of the electric field based on 250 investigated cases.

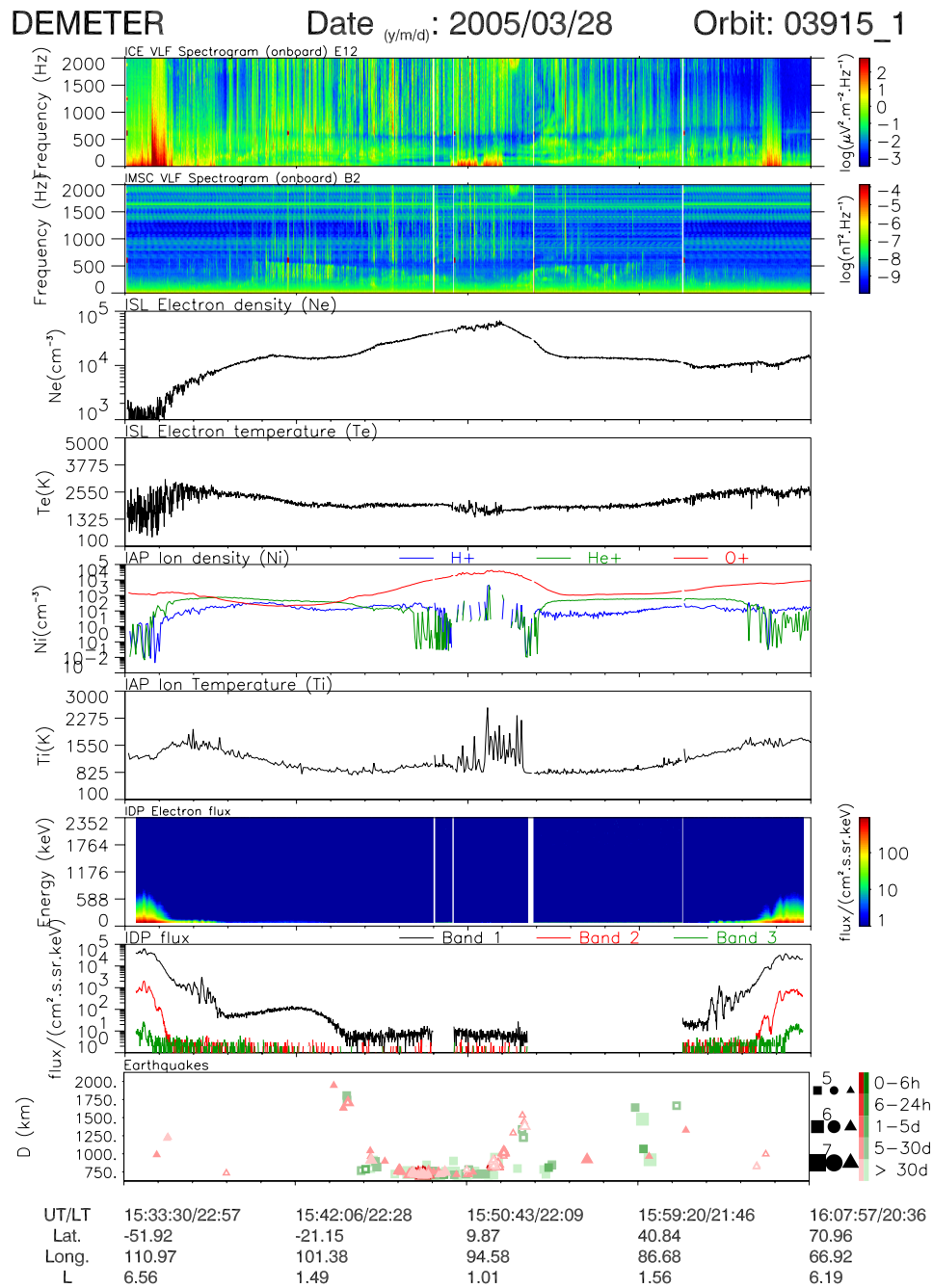


Fig. 1. The electromagnetic perturbations before the Sumatra 8.6 Earthquake on 28 March 2005.

DEMETER, a French micro-satellite, launched on 29 June 2004, was the first one in the world to be designed specially for studying the ionospheric variations possibly associated with earthquakes, man made transmitters, volcanoes and lightning, having a solar synchronous circular orbit, declination of 98.23°, and a height of 710 km (which decreased to 660 km in mid-December 2005). A set of instruments were

deployed on the satellite, including ICE to detect the electric field from DC to 3.5 MHz; IMSC to measure the magnetic field from a few Hz to 20 kHz; IAP to detect ion density and temperature; ISL, Langmuir probe to measure the electron density and temperature; IDP to detect the energetic electron flux at 72.9 keV–2.34 MeV.

As for the study about DEMETER satellite, Parrot et al. (2006) firstly showed examples of ionospheric perturbations in the electron density, electric and magnetic field, and high energy particles before some strong earthquakes. Némec et al. (2009) present their results that the power spectra density in the ELF/VLF electric field decreased 0–4 h before the main shocks at the frequency 1.7 kHz during local nighttime. Athanasiou et al. (2011) studied the ULF electromagnetic waves around the Haiti $M = 7.0$ earthquake, and they exhibited the variations of the E_z -electric field component during a time period of 100 days before and 50 days after it. Their results showed a significant increase in energy E_z for the time interval of 30 days before this earthquake. In some case studies, an interesting phenomenon of electrostatic perturbation was observed in the electric field at a frequency lower than 250 Hz before some strong earthquakes (Zhang et al., 2009; Ouyang et al., 2007), in which the electrostatic perturbations appeared where they rarely occurred over regions at mid- and lower-latitude of 20–35°. In this paper, we are focusing on, in more detail, the electric field data in the nighttime observed by DEMETER around the earthquakes of $M_s \geq 7.0$ in globe since 1 January 2005 to 28 February 2010. The electrostatic perturbations in the ionosphere are picked up and analysed. The coupling mechanism between earthquakes and ionospheric electrostatic perturbations is discussed as well.

2 Data collection and anomaly identification

Due to incomplete orbits at the end half of 2004, the beginning stage of DEMETER, the satellite data during this period was not included in this paper. A total of 69 strong earthquakes above a magnitude 7.0 since January of 2005 to February 2010 were collected (<http://neic.usgs.gov>; <http://www.csndmc.ac.cn>). If the earthquake with a magnitude above 7.0 is dealt with, the scope of the so called “seismic preparation region” could exceed 1000 km from the epicentre expressed in terms of the equation of $\rho = 10^{0.43M}$ based on the statistics of the ground observation (Dobrovosky et al., 1979) within the scope, some ionospheric perturbations could possibly be triggered by the earthquake preparation process. The observing satellite data were chosen during the 9 days with 7 days before and 1 day after these earthquakes. It should be noted that ULF electromagnetic activity was detected much earlier and probably suggests a long period of ULF seismic precursory signals (Hayakawa et al., 1996). Here, we focused on short-term ULF/ELF phenomena after considering the conclusions about ionospheric precursors that occurred mostly within a week before the earthquakes (Pulinets and Boyarchuk, 2004). Only up-orbits recorded during nighttime, under quiet electromagnetic condition, were selected in this paper to avoid the effects of solar activity. Taking into account the spatial correlation, the anomalies could be considered to be related to the earth-

quakes if they occurred at a latitude scale within $\pm 10^\circ$ relative to the epicentre latitude, because whatever the direct projection position of the epicentre or signals propagating along the magnetic field line from the focal area may not exceed more than 10° in latitude over the mid-low latitude regions. The pictures in the paper of Gousheva et al. (2008) also verify that ULF electric field anomalies in the ionosphere were distributed over the seismic regions, sometimes extending far from the epicentral latitudes. In order to ensure that at least one orbit of the DEMETER satellite can be found every day over a certain region, the up-orbits were chosen within the distance of 2000 km to the epicentre in longitude.

The orbit (3915-1) in Fig. 1 is such an example of anomalies chosen according to the requirement, just flying over Indonesia 50 min before the Sumatra $M = 8.6$ Earthquake occurring at 16:39:36.52, 28 March 2005, located at $97.11^\circ\text{E} - 2.09^\circ\text{N}$. In Fig. 1, the panels show the parameters (from top to bottom) as follows: the VLF electric field spectrum at 19.5 Hz–2 kHz, the VLF magnetic field spectrum at 19.5 Hz–2 kHz, N_e (electron density), T_e (electron temperature), N_i (ion density of H^+ , He^+ , O^+), T_i (ion temperature), the energetic electron spectrum between 72.9 keV–2.34 MeV, the electron flux at three bands (90–600 keV; 0.6–1 MeV; 1–2.34 MeV), the earthquakes occurring less than 2000 km apart from this orbit during ± 30 days. As presented in Fig. 1, the disturbances were detected at the equatorial region in most observing parameters, including the electric field at ULF/ELF frequency band that we paid attention to in this paper, electron density, electron temperature, ion density, and so on. Here the perturbations, at ULF/ELF band less than 250 Hz of the electric field, are considered as electrostatic perturbations.

Figure 2 exhibits the disturbances extracted from the electric field spectrum along orbit 3915-1. The first top panel presents the median value of PSD (power spectrum density) in the electric field at 19.5–250 Hz, in which the spectra density over the seismic region increased with two orders of magnitude relative to its surrounding normal level, exceeding $10^2 \mu\text{V}^2/\text{m}^2/\text{Hz}$. After repetitive testing, the electrostatic perturbations were selected by an automatic technique developed by Zhang et al. (2010). They were picked following this definition: $A_0 > 10^{0.7} \mu\text{V}^2/\text{m}^2/\text{Hz}$ where A_0 is the first PSD value at 19.5 Hz, and other PSD values at the following frequency points should fit the exponential relation of $S_E = A_0 \cdot f^{-b}$, where S_E represents the PSD value at a different frequency and f is frequency (Zhang et al., 2010). The lower panel shows the selected anomalous signals (with value 1) and normal points (with value 0). It can be found that the distinguished anomalies are consistent with the perturbations shown in the top panel. In Fig. 2, some strong perturbations were also very clear and significantly above the latitude of 40° , which can be detected almost every day, especially along the orbits of the Eastern Hemisphere. So these perturbations at higher latitudes may not be related to strong earthquakes, but to the auroral electrojets and energetic electrons precipitation into radiation belts over

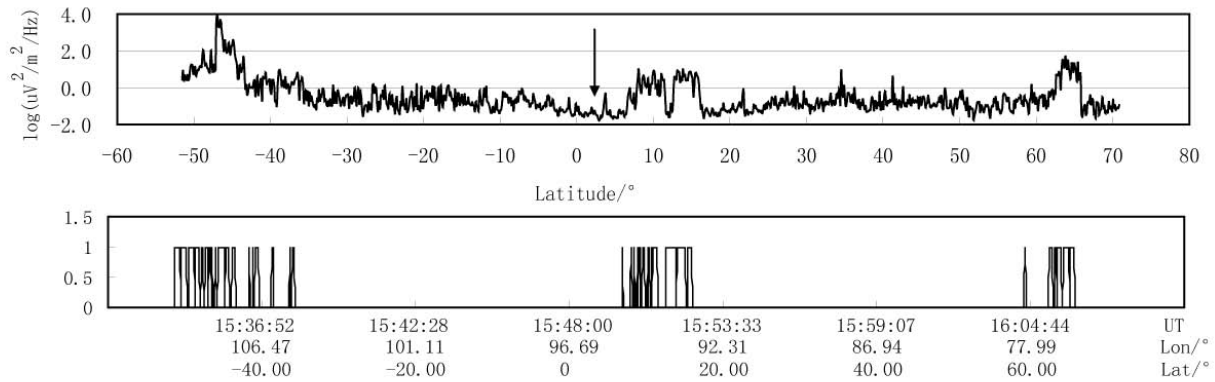


Fig. 2. Ionospheric perturbations in electric field along the orbit 3915-1.

this region, which can be proven by the stronger particle flux at the same latitudes. These signals at high latitudes should be cast off in anomaly identification according to their geographical positions, therefore, earthquakes at high latitudes were not discussed in this paper because it is difficult to distinguish whether or not the perturbations in the electric field were motivated by earthquakes under this strong noise background.

Based on the definition of anomalies and electrostatic perturbations, among 69 earthquakes within the latitude of 40° , the electrostatic perturbations were observed before the 32 earthquakes along the up-orbits in a distance from the epicentres less than 2000 km during the 9 days, while there is one earthquake only showing post-seismic anomaly without precursors. All the details about these 32 earthquakes and anomalies around them are listed in Table 1, including the date, time, magnitude(Ms), longitude(Lon), latitude(lat), depth of the earthquake and also the time differences between anomalies and earthquakes, latitude and longitude scale of anomalies, median value of PSD in the electric field at 19.5–250 Hz, and daily $\sum Kp$ index. Some of the $\sum Kp$ values are followed by the letter D that represents that day being in a disturbed state. Actually, the Kp in most days was not marked by D in Table 1, which means most anomalies appeared in quiet electromagnetic condition. It also demonstrated, from another aspect, that the perturbations could be well correlated with earthquakes, instead of solar activity or other space impact-factors due to low Kp values during those days.

It can be seen from Table 1 that the anomalies in ULF/ELF electric field appeared many times before some earthquakes, such as the Sumatra 8.6 Earthquake on 28 March 2005; Haiti 7.0 Earthquake on 12 January 2010 and so on, which reflect that ULF/ELF perturbations continued a long time over the seismic region during the earthquake preparation process. Moreover, there are 21 earthquakes among 32 events with the ionospheric perturbations occurring in 3 days prior to them, showing the short-term temporal feature of ULF/ELF EM perturbations in ionosphere.

3 Analysis on electrostatic perturbations and discussion

3.1 Spatial distribution of earthquakes

Figure 3 shows the global epicentral distribution of the selected 32 earthquakes (Fig. 3a), and the projection of their depths versus latitudes (Fig. 3b). It can be seen that: (1) these earthquakes are mostly located at the plate boundaries; (2) there are 21 earthquakes located in the latitude scale of $\pm 20^\circ$, with electrostatic perturbations being unusual; (3) among them 8 earthquakes are deeper than 100 km, occupying 25 %, and even most earthquakes are located in the ocean, not on land, as shown in Table 1. Figure 3a shows that these 32 earthquakes are mainly along the Circum-Pacific Seismic belt, which may indicate that interaction between giant plates would more easily produce intensive anomalies along the major faults and then induce electrostatic perturbations in the ionosphere.

It is well known that when EM waves propagate in water from the ocean bottom, they will attenuate largely, that is to say, the EM wave has difficulty when penetrating seawater into the atmosphere and ionosphere directly. Why so many perturbations were detected before oceanic earthquakes? A speculation might explain it as follows: radon or other chemical materials emitted from the oceanic faults would change the ionization in seawater and the composition of water ions in it. This change would lead to the variation of the atmospheric vertical electric field over the seismic region. The variation of atmospheric electric field as a part of the current system between ionosphere and lithosphere would cause the change of the current system in the ionosphere, which might lead to the disturbances in kinds of parameters including the ULF/ELF electric field.

Table 1. Summary of anomalous information in ULF/ELF electric field related to strong earthquakes.

Date y-m-d	Time h-m-s	Ms	Lon /°E	Lat /°N	Depth /km	Land or Ocean	Δt T-Te	Latitude scale of anomalies	Longitude scale of anomalies	Median value /lg($\mu\text{V}^2/\text{m}^2/\text{Hz}$)	Kp
2010-02-27	06-34-16.4	8.8	-72.7	-35.8	33	L	-3 day -2 day	39°~42°S 39°~41°S	298.5°~299.5°E 291°~292°E	1 0.5	6 6
2010-1-12	21-53-09.85	7.0	-72.53	18.46	10	L	-5 day -1 day +1 day	23°~26°N 5°~20°N 10°~21°N	302.5°~303°E 273°~275°E 282°~286°E	0~1 0~1 0~0.5	1 13 14(D)
2010-1-3	22-36-28.15	7.2	157.3	-8.9	25	O	-12 h	4°~12°S	168°~169.5°E	0.5	7
2009-10-7	22-18-51.24	7.8	166.38	-12.52	35	O	-1 day	1°~9°S	176°~177.5°E	0.5~1	3
2009-9-29	17-48-10.99	8.1	-172.1	-15.49	18	O	-5 day	6°~10°S	194°~195°E	1~2	2
2009-9-2	07-55-01.05	7	107.3	-7.78	46	O	-2 day	10°~16°S	106°~107°E	0~0.5	11
2009-8-10	19-55-35.61	7.5	92.89	14.1	4	O	-1 day	12°~14°N	95°~96°E	0~1	12
2009-8-9	10-55-55.61	7.1	137.94	33.17	297	O	-4 day +1 h	35°~43°N 32°~37°N	117°~120°E 138°~140°E	1 0.5	11 12
2009-3-19	18-17-40.91	7.6	-174.66	-23.05	34	O	-6 day -1 day	17°~24°S 18°~20°S	169°~171°E 180°~181°E	0.5~1 0.5	25(D) 3
2009-2-18	21-53-45.16	7.0	-176.33	-27.42	25	O	-5 day -4 day -2 day -18.5 h	10°~21°S 12°~20°S 16°~28°S 18°~26°S	182°~185°E 175°~177°E 185°~188°E 195°~197°E	0.5~1.2 1 1 0.5	4 24(D) 7 6
2009-2-11	17-34-50.49	7.2	126.39	3.89	20	O	-3 day +1 day	6°S~2°N 0°~5°N	119°~121°E 137°~138°E	0.5 0.5~1.0	1 3
2008-4-9	12-46-12.72	7.3	168.89	-20.07	33	O	-5 day -2 h	12°~20°S 16°~21°S	159°~161°E 170°~171.5°E	0.4 0.5	15 22
2007-12-9	07-28-20.82	7.8	-177.51	-26	152	O	-7 day -5 day -3 day -2 day	18°~19°S 28°~35°S 20°~30°S 24°~32°S	179°~180°E 191°~193°E 175°~200°E 190°~200°E	1.5 1~1.5 0.5~1.2 0.5~1.2	3 2 5 2
2007-11-29	19-00-20.42	7.4	-61.27	14.94	156	O	-5 day	4°~6°N	309°~309.5°E	0~1	22(D)
2007-11-14	15-40-50.53	7.7	-69.89	-22.25	40	L	-6 day -3 day -1 day	24°~37°S 25°~40°S 10°~23°S	291°~295°E 294°~297°E 299°~301°E	0 0 -1~0	7 4 19
2007-9-12	11-10-26.83	8.5	101.37	-4.44	34	L	-5 day -5.7 h	4°~10°S 8°~10°S	100°~101°E 111°~112°E	0.7~1.5 0.3	18 4
2007-9-2	01-05-8.15	7.2	165.76	-11.61	35	O	-5 day -4 day	6°~16°S 5°~20°S	177°~179°E 169°~173°E	0.5~1 0.5~1	18 9
2007-08-15	23-40-57.89	8.0	-76.6	-13.39	39	L	-6 day	8°~12°S	298.5°~299.3°E	0.5	6
2007-8-8	17-05-04.92	7.5	107.42	-5.86	280	O	-4 day -2 day -2 h	1°S~5°N 4°~9°S 4°S~5°N	113°~115°E 100°~101°E 107°~110°E	0.5~1.2 0.5~1 0.5~1	2 18 11
2007-8-1	17-08-51.4	7.2	167.68	-15.6	120	O	-6 day	10°~20°S	161°~163°E	0.5~1.5	13
2007-4-1	20-39-58.71	7.2	157.04	-8.47	24	O	-4 day	6°~10°S	149°~150°E	0.5~1.5	12
2007-3-25	00-40-1.61	7.1	169.36	-20.62	34	O	-7 day -5 day	4°~15°S 4°~18°S	151°~154°E 161°~164°E	0.5 0.5~1.5	6 1
2006-7-17	08-19-30.5	7.3	107.4	-9.4	20	O	-7 day -6 day -5 day -4 day -3 day +7 h	18°~20°S 14°~20°S 14°S~6°N 20°S~20°N 20°S~20°N 14°~20°S	116.5°~117°E 108°~110°E 96°~101°E 90°~120°E 100°~115°E 111°~113°E	1 1 0~1 0~1 1 1~1.5	17 12 19(D) 10 19(D) 6
2006-5-16	15-28-24.6	7.2	97.2	0.1	12	O	-1 h= +0.5 h	2°S~2°N 8°~10°S	117°~118°E 94°~96°E	0.5~1 0.4~1	6 6
2006-5-16	10-39-20.4	7.4	-179.31	-31.81	152	O	-1 h	33°~35°S	198°~200°E	0.5~1	6
2006-2-22	22-19-9.6	7.5	33.2	-21.1	11	L	-3 day	9°~12°S	42°~43°E	0.5~1	14
2006-1-27	16-58-50.0	7.6	128.1	-5.4	397	O	-2.5 h	2.8°S~15°N	115°~120°E	0~1	20
2005-9-26	01-55-37.67	7.5	-76.4	-5.68	115	L	-4 day -3 day	14°~25°S 10°~23°S	276°~279°E 290°~296°E	1 1	13 12
2005-9-9	07-26-43.73	7.6	153.47	-4.54	90	O	-5 day -4 day -3 day -1 day +3.5 h	6°~10°S 4.5°~6°S 10°S~10°N 6°~10°S 4°~13°S	147°~148°E 160.5°~161°E 144°~154°E 153.5°~154.5°E 167°~169°E	0.5~1 0.4~0.6 0.5~1 0.5~1 0.4~1	29 20 15 13 22
2005-08-16	02-46-28.4	7.2	142.04	38.28	36	L	+1 day	37°~41°N	157°~159°E	0~1	22
2005-07-24	15-42-06.21	7.2	92.19	7.92	16	O	-2 day	14°~15°N	80°~81°E	0.5~1	20
2005-3-28	16-09-36.53	8.6	97.11	2.09	30	L	-6 day -5 day -3 day -20 min	1°S~4°N 6°S~2°N 8°~11°N 3.5°~14.8°N	109°~110°E 101°~103°E 102°~103°E 93°~95°E	1~1.5 0.5~1 0.3 0.5~1	5 7 27(D) 9

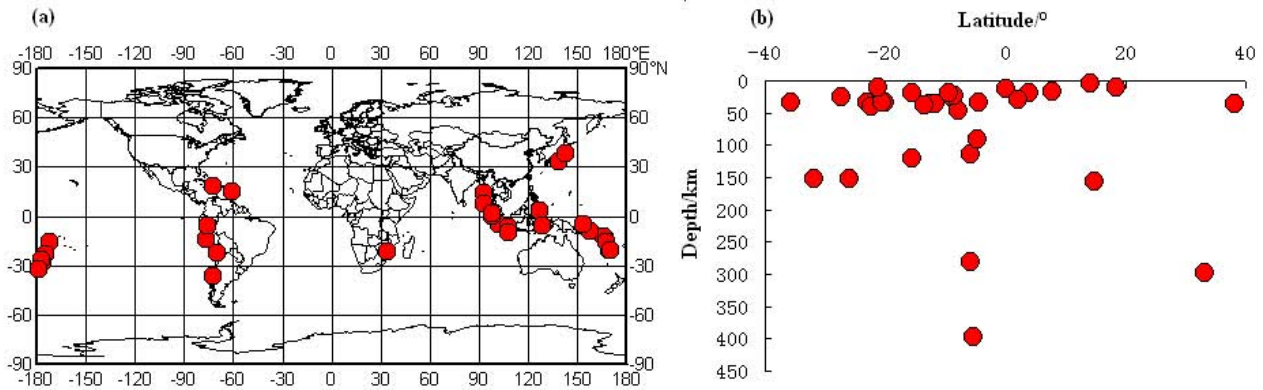


Fig. 3. Spatial (a) and depth (b) distribution of earthquakes with electrostatic perturbations (the circle represents the earthquake).

3.2 Extended spatial characteristic of ULF/ELF electric field perturbations

In order to study the relationship between ULF/ELF electrostatic perturbations and earthquakes, the global distribution of the perturbations before the Sumatra $M = 8.6$ Earthquake on 28 March 2005 were selected as an example and the time differences were still limited to 7 days before the earthquakes as mentioned above. As shown in Table 1, the perturbations appeared on 22, 23, 25 and 28 March in the orbits within the range of 2000 km from the epicentre. Here the question is whether the anomalies in the ionosphere only occur at the orbits nearest to the epicentre, or also at other orbits. Take the Sumatra Earthquake on 28 March 2005 as an example, the black segments marked in Fig. 4 give the global distribution of EM perturbations during those days except the ones on 25 March which might be influenced by magnetic storms on that day. To allow a convenient comparison and visualized figures, the electric field signals with PSD larger than $5 \mu\text{V}^2 \cdot \text{m}^{-2} \cdot \text{Hz}^{-1}$ and fitting exponential delay laws at the low frequency band of 19.5–250 Hz (Zhang et al., 2010) were assigned values of 1 (black circles) and taken as a time segment of perturbations, or else they would be assigned values of 0 (gray circles) and taken as a time segment without disturbances. All the perturbations at the ultra-low frequency band are picked up along the orbits and plotted in Fig. 4. It can be seen that, at the latitude higher than 40° , there existed lots of these ULF/ELF perturbations, reasonably due to the effects of the polar ring current, energetic electron precipitation and other factors, which can also be seen very clearly in Figs. 1 and 2. Besides those signals at high latitudes, one could, however, find many perturbations around the epicentre of this $M = 8.6$ earthquake (black triangle) at lower latitudes in the range of $\pm 20^\circ$, and they extended from 0° to 150° E on 22 and 23 March. While, the perturbations on 28 March only occurred at the orbit closest to the epicentre, which shows a different feature with those on 22 and 23.

Similar EM perturbations, with a large scale, were also found before some other earthquakes (Zhang et al., 2010; Ruzhin et al., 1998). It seems to the authors that the following hypothesis of taking the stress changes during the earthquake preparation process as a source corresponding to the perturbations in the ionosphere, would be helpful in understanding the feature. During the seismic preparation stage, there would be a region much larger than the epicentral area, being under a state of stress accumulation, and the electromagnetic signals might be frequently produced and continue for a long time. When they propagate to the ionosphere, together with the ion and electron drift in the ionosphere, they can be detected by many orbits. As soon as the earthquake process enters into its impending stage, the stress would be concentrated just in the epicentral area while the anomalous region would shrink correspondingly.

3.3 Discussion

The possible coupling mechanisms among lithosphere-atmosphere-ionosphere (LAI) have been suggested in many publications (Pulinets et al., 2000; Pulinets and Boyarchuk, 2004; Molchanov et al., 2004; Rycroft, 2006; Namgaladze et al., 2009; Pulinets and Ouzounov, 2011). Some of them will be discussed on the ionospheric perturbations in the ULF/ELF electric field associated with strong earthquakes.

One possible mechanism is the direct penetration of ULF/ELF EM waves from the epicentres into the ionosphere. There are many results to illustrate the existence of ULF/ELF/VLF electromagnetic (EM) emissions prior to strong earthquakes in ground-based observations (Hayakawa, 2004). When energy is accumulated underground to some extent, microstructures will increase and electromagnetic emissions will be produced simultaneously. Another source has also been proposed that positively charged holes are easy to constitute into minerals especially semi-conductor minerals when they are heated. Some laboratory experiments support this possibility (Freund, 2000; Shen et al., 2009). Based on numerical computations, ULF/ELF

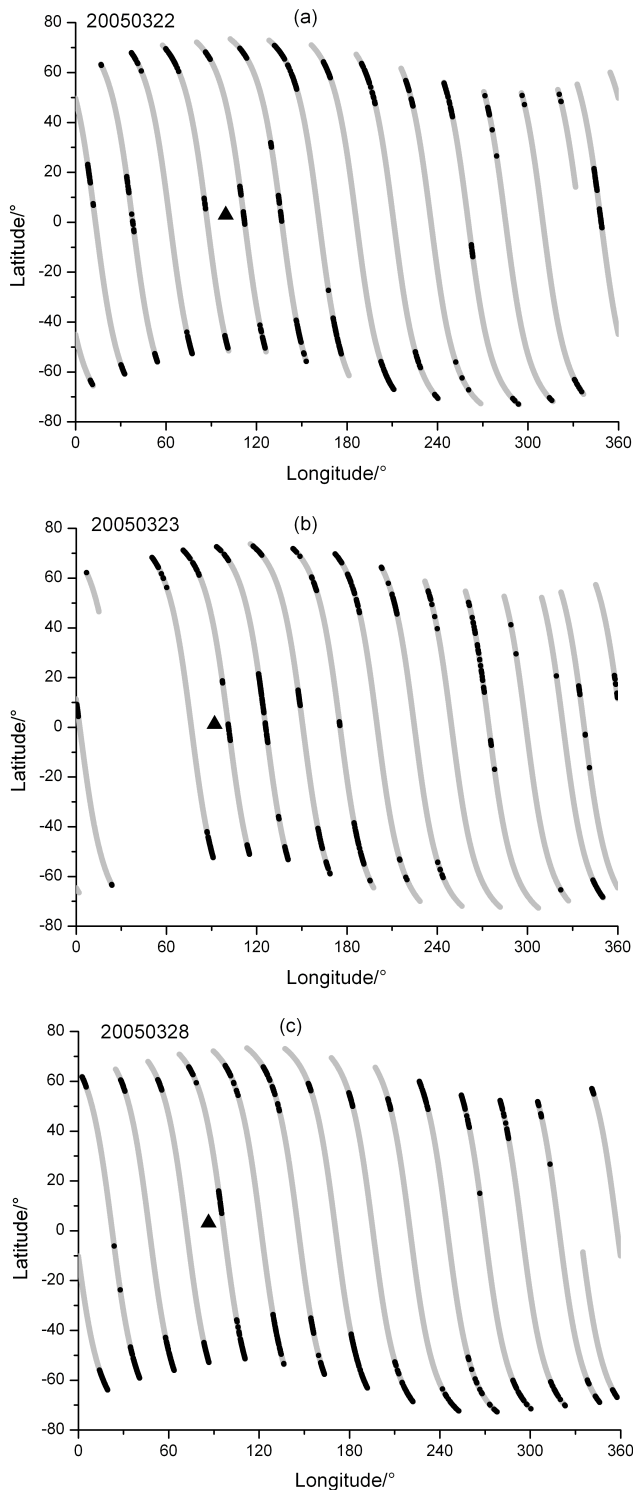


Fig. 4. The spatial distribution of electrostatic perturbations (dark points) on 22, 23 and 28 March before a 8.6 earthquake at Sumatra Indonesia on 28 March 2005 (the triangle in the figure is the epicentre).

electromagnetic emissions lower than 20 Hz can transverse directly into the upper ionosphere by penetrating or non-penetrating solutions with a decrease of an order of magnitude (Bortnik and Bleier, 2004). The transverse electric (TE) component of ULF noises is transformed into Alfvén waves at the atmosphere-ionosphere boundary, and nonlinear interactions of ULF Alfvén waves with energetic particles in the magnetosphere may result in the occurrence of ELF/VLF emissions in the upper ionosphere (Larkina et al., 1989; Molchanov et al., 1993).

Another one is that the enhanced Equatorial Ionospheric Anomaly (EIA) may also induce electrostatic (ES) turbulences (Namgaladze et al., 2009). The heating of sunlight and tidal effects will lead to the upward movement of plasma in the lower ionosphere, penetrating the geomagnetic power lines and then constructing an electric current in E layer. This electric current acts with horizontal magnetic power lines and causes the increase in electron density in the ionosphere at $\pm 20^\circ$ geomagnetic latitudes around the magnetic equator. In our paper, at the observing altitude of DEMETER with 660–710 km, the ionospheric crest is always shown as one peak near the magnetic the equatorial area (see the first panel of electron density in Fig. 1), but as shown in Fig. 4 and combined with the results of Pulinetz et al. (2006), the perturbations occurred at two sides of the crest of Ne on 22 and 23 March before the Sumatra Earthquake. Over an epicentral area near the equator, the vertical electric field might be changed due to the accumulation of radon or aerosols in the near-earth atmosphere at the seismic preparation area (Liperovsky et al., 2005), and then the east directed polarization electric field would be generated due to the different drift velocities of electrons and ions. The east directed electric field would stimulate the equatorial anomaly amplification while plasma bubble would be formed in the bottom-side ionosphere and float up to the DEMETER altitude (Pulinetz et al., 2006). The double peak structure can persist until the late evening hours, just the time of the DEMETER up-orbits in local nighttime, which has been recently proven in the paper of Vyas and Andamandan (2011). So this mechanism may be used to explain some anomalous phenomena in ULF/ELF electric field near the equatorial area.

4 Conclusions

Among 69 earthquakes, DEMETER satellite observed ionospheric perturbations in the ULF/ELF electric field during local nighttime before the 32 earthquakes, which demonstrates that these ionospheric disturbances were not casual phenomena, but may be associated with earthquakes. All the characteristics of these anomalies were summed up as follows:

1. Before 46 % strong earthquakes in 69 studied cases with a magnitude above $M_s = 7.0$, the electrostatic perturbations were obtained at 19.5–250 Hz in a distance of

2000 km and latitudinal difference of 10° in the ionosphere. The anomalies occurred mostly within 3 days before the 21 earthquakes. Only 7 earthquakes among them showed anomalies a few hours before the earthquakes (Table 1). These 32 earthquakes are mainly located at the boundary of plates. But the depth of earthquakes does not show significant influence on the forming of ES turbulences in the ionosphere.

- Extended study in this paper proved that before the 8 earthquakes, the perturbations in the ionosphere could be observed in a very large scale in longitude, but when the observing time was closer to the earthquake occurrence, the anomalous area shrank, and perturbations always only occurred along the closest orbits apart from the epicentres, which may be related to the different stress developing stages in the earthquake preparation process.
- There are 54% of earthquakes with no obvious ES perturbations detected. The main reasons that are taken into account: the first, some of these cases are located at high latitudes so the ES perturbations can not be easily distinguished with those long existing ES turbulences at this region; the second, the flying time of a single satellite is limited when it crosses a certain place, only once a day like the DEMETER satellite, so it can not be ensured that the anomaly at the seismic region can continue for a very long time in order to meet the satellite; the third, there was no anomaly at all at the seismic region, or the anomaly is not intense enough to result in ionospheric perturbations.
- The LAI coupling process is complex and there are only some qualitative interpretations at present. Based on the results in this paper and combined with other researches, the direct ULF/ELF EM propagation, the coupling mechanism between the enhanced vertical electric field in the atmosphere and EIA amplification are suggested to be important factors to explain the ionospheric electrostatic perturbations in the ULF/ELF electric field. In order to understand and verify the mechanism between the ionospheric perturbations with strong earthquakes, it is necessary to strengthen the observation of multi-parameters on the ground, in the atmosphere and ionosphere synchronously.

Acknowledgements. This paper is funded by the International Cooperation Project (2009DFA21480) and the Key Earthquake Science Research Fund (201008007). We are grateful to the DEMETER Data Centre for the provision of the satellite data.

Edited by: M. E. Contadakis

Reviewed by: three anonymous referees

References

- Anagnostopoulos, G. and Rigas, V.: Variations of energetic radiation belt electron precipitation observed by DEMETER before strong earthquakes, *Geophys. Res. Abstr.*, EGU2009-10700, 11, 2009.
- Athanasίου, M. A., Anagnostopoulos, G. C., Iliopoulos, A. C., Pavlos, G. P., and David, C. N.: Enhanced ULF radiation observed by DEMETER two months around the strong 2010 Haiti earthquake, *Nat. Hazards Earth Syst. Sci.*, 11, 1091–1098, doi:10.5194/nhess-11-1091-2011, 2011.
- Bortnik, J. and Bleier, T.: Full wave calculation of the source characteristics of seismogenic electromagnetic signals as observed at LEO satellite altitudes, *Eos Trans. AGU*, 85(47), Fall Meet. Suppl., Abstract T51B-0453, 2004.
- Dobrovosky, I. R., Zubkov, S. I., and Myachkin, V. I.: Estimation of the size of earthquake preparation zones, *PAGEOPH*, 117, 1025–1044, 1979.
- Freund, E.: Time-resolved study of charge generation and propagation in igneous rocks, *J. Geophys. Res.*, 105, 11001–11019, 2000.
- Gousheva, M., Danov, D., Hristov, P., and Matova, M.: Quasi-static electric fields phenomena in the ionosphere associated with pre- and post earthquake effects, *Nat. Hazards Earth Syst. Sci.*, 8, 101–107, doi:10.5194/nhess-8-101-2008, 2008.
- Hayakawa, M.: Electromagnetic phenomena associated with earthquakes: a frontier in terrestrial electromagnetic noise environment, *Recent Res. Dev. Geophys.*, 6, 81–112, 2004.
- Hayakawa, M., Molchanov, O. A., Ondoh, T., and Kawai, E.: The precursor signature effect of the Kobe earthquake in VLF subionospheric signal, *J. Comm. Res. Lab., Tokyo*, 43, 160, 1996.
- Larkina, V. I., Migulin, V. V., Molchanov, O. A., Kharkov, I. P., Inchin, A. S., and Schvetcova, V. B.: Some statistical results on very low frequency radiowave emissions in the upper ionosphere over earthquake zones, *Phys. Earth Planet. In.*, 57, 1–2, 100–109, 1989.
- Liperovsky, V. A., Meister, C.-V., Liperovskaya, E. V., Davidov, V. F., and Bogdanov, V. V.: On the possible influence of radon and aerosol injection on the atmosphere and ionosphere before earthquakes, *Nat. Hazards Earth Syst. Sci.*, 5, 783–789, doi:10.5194/nhess-5-783-2005, 2005.
- Molchanov, O. A., Mazhaeva, O. A., Goliavin, A. N., and Hayakawa, M.: Observation by the Intercosmos-24 satellite of ELF-VLF electromagnetic emissions associated with earthquakes, *Ann. Geophys.*, 11, 431–440, 1993, <http://www.ann-geophys.net/11/431/1993/>.
- Molchanov, O., Fedorov, E., Schekotov, A., Gordeev, E., Chebrov, V., Surkov, V., Rozhnoi, A., Andreevsky, S., Iudin, D., Yunga, S., Lutikov, A., Hayakawa, M., and Biagi, P. F.: Lithosphere-atmosphere-ionosphere coupling as governing mechanism for preseismic short-term events in atmosphere and ionosphere, *Nat. Hazards Earth Syst. Sci.*, 4, 757–767, doi:10.5194/nhess-4-757-2004, 2004.
- Namgaladze, A. A., Klimenko, M. V., Klimenko, V. V., and Zakharenkova, I. E.: Physical mechanism and mathematical modeling of earthquake ionospheric precursors registered in total electron content, *Geomagn. Aeronomy+*, 49, 2, 252–262, 2009.
- Němec, F., Santolík, O., and Parrot, M.: Decrease of intensity of ELF/VLF waves observed in the upper ionosphere close to

- earthquakes: A statistical study, *J. Geophys. Res.*, 114, A04303, doi:10.1029/2008JA013972, 2009.
- Ouyang, X. Y., Zhang, X. M., Shen, X. H., Liu, J., Qian, J. D., Cai, J. A., Zhao, S. F.: Ionospheric Ne disturbances before 2007 Pu'er Yunnan China earthquake, *Acta Seismologica Sinica*, 21(4), 425–437, 2008.
- Parrot, M.: Statistical study of ELF/VLF emissions recorded by a low-altitude satellite during seismic events, *J. Geophys. Res.*, 99(A12), 23339–23347, 1994.
- Parrot, M., Berthelier, J. J., Lebreton, J. P., Sauvaud, J. A., Santolík, O., and Blecki, J.: Examples of unusual ionospheric observations made by the DEMETER satellite over seismic regions, *Phys. Chem. Earth*, 31, 486–495, doi:10.1016/j.pce.2006.02.011, 2006.
- Parrot, M. and Mogilevsky, M. M.: VLF emissions associated with earthquakes and observed in the ionosphere and the magnetosphere, *Phys. Earth Planet. In.*, 57, 1–2, 86–99, 1989.
- Pulinets, S. A., Boyarchuk, K. A., Hegai, V. V., Kim, V. P., and Lomonosov, A. M.: Quasielectrostatic model of atmosphere-thermosphere-ionosphere coupling, *Adv. Space Res.*, 26, 1209–1218, 2000.
- Pulinets, S. A. and Boyarchuk, K. A.: *Ionospheric Precursors of Earthquakes*, Springer, Berlin, Heidelberg, New York, 1–287, 2004.
- Pulinets, S. and Ouzounov, D.: Lithosphere-Atmosphere-Ionosphere Coupling(LAIC) model-An unified concept for earthquake precursors validation, *J. Asian Sci.*, 41, 371–382, 2011.
- Pulinets, S., Ouzounov, D., and Parrot, M.: Conjugated near-equatorial effects registered by DEMETER satellite before Sumatra earthquake $M = 8.7$ of March 28, 2005, *International Symposium of DEMETER*, Toulous-France, 14–16 June 2006.
- Ruzhin, Y. Y., Larkina, V. A., and Depueva, A. K.: Earthquake precursors in magnetically conjugated ionosphere regions, *Adv. Space Res.*, 21, 525–528, 1998.
- Rycroft, M. J.: Electrical processes coupling the atmosphere and ionosphere: An overview, *J. Atmos. Solar-Terr. Phys.*, 68, 445–456, 2006.
- Serebryakova, O. N., Bilichenko, S. V., Chmyrev, V. M., Parrot, M., Rauch, J. L., Lefeuvre, F., and Pokhotelov, O. A.: Electromagnetic ELF radiation from earthquake regions as observed by low-altitude satellites, *Geophys. Res. Lett.*, 19, 91–94, 1992.
- Shen, J. F., Shen, X. H. and Liu, Q.: Thermoelectricity property of natural semi-conductor minerals and its application in earthquake prediction, *Bulletin of Mineralogy, Petrology and Geochemistry*, 28, 301–307, 2009, (in Chinese with English Abstract).
- Vyas, B. M. and Andamandan B.: Nighttime VHF ionospheric scintillations characteristic near the crest of Appleton anomaly station Udanpur (24.6° N, 73.7° E), *Indian J. Radio Space*, 40, 191–202, 2011.
- Zhang, X., Battiston, R., Shen, X., Zerenzhima, Ouyang, X., Qian, J., Liu, J., Huang, J., and Miao, Y.: Automatic collecting technique of low frequency electromagnetic signals and its application in earthquake study, in: *Knowledge Science, Eng. Manag.*, edited by: Bi, Y. and Williams, M. A., KSEM2010, LANI 6291, Springer, Berlin, Heidelberg, 366–377, 2010.
- Zhang, X., Qian, J., Ouyang, X., Shen, X. H., Cai, J. A., and Zhao, S. F.: Ionospheric electromagnetic perturbations observed on DEMETER satellite before Chile M7.9 earthquake, *Earthquake Sci.*, 22, 251–255, 2009.
- Zhang, X., Zhao, G. Z., Chen, X. B., and Ma, W.: Seismo-electromagnetic observation abroad, *Prog. Geophys.*, 22, 3, 687–694, 2007 (in Chinese with English Abstract).